

A New Polar Code Design Based on Reciprocal Channel Approximation

Hideki Ochiai, Kosuke Ikeya, and Patrick Mitran

Abstract

This paper revisits polar code design for a binary-input additive white Gaussian noise (BI-AWGN) channel when successive cancellation (SC) decoding is applied at the receiver. We focus on the *reciprocal channel approximation (RCA)*, which is often adopted in the design of low-density parity-check (LDPC) codes. In order to apply RCA to polar code design for various codeword lengths, we derive rigorous closed-form approximations that are valid over a wide range of SNR over an AWGN channel, for both the mutual information of BPSK signaling and the corresponding *reciprocal channel mapping*. As a result, the computational complexity required for evaluating channel polarization is thus equivalent to that based on the popular Gaussian approximation (GA) approach. Simulation results show that the proposed polar code design based on RCA outperforms those based on GA as well as the so-called improved GA (IGA) approach, especially as the codeword length is increased. Furthermore, the RCA-based design yields a better block error rate (BLER) estimate compared to GA-based approaches.

Index Terms

Code construction, density evolution, Gaussian approximation, polar codes, reciprocal channel approximation.

I. INTRODUCTION

One of the most striking properties of polar codes [1] is their capacity approaching behavior that is achievable with low-complexity successive cancellation (SC) decoding. Specifically, for a codeword length of N bits, the decoding complexity is only $O(N \log N)$, which is significantly lower than other known capacity approaching codes that are available in practice. As a result of channel polarization, the design of polar codes is equivalent to the identification of good channels and bad channels, where the former channels are used for information transmission and the latter

H. Ochiai and K. Ikeya are with the Department of Electrical and Computer Engineering, Yokohama National University, Yokohama, Japan. (email: hideki@ynu.ac.jp, ikeya-kosuke-fc@ynu.jp)

P. Mitran is with the Department of Electrical and Computer Engineering, University of Waterloo, ON, Canada. email:pmitran@uwaterloo.ca

channels are left unused (i.e., *frozen*). The main focus of this paper is on the design of polar codes with various codeword lengths over a binary-input additive white Gaussian noise (BI-AWGN) channel.

There have been various techniques proposed for polar code design over a BI-AWGN channel. The most accurate analytical approach is the use of density evolution [2, 3], originally developed for the design of low-density parity-check (LDPC) codes, and its applicability to polar codes has been identified in [4]. Density evolution tracks the probability distribution of the channel or its log-likelihood ratio (LLR), and in order to improve its accuracy, it should be computed with sufficient quantization and dynamic range. Therefore, density evolution is highly demanding in terms of space and computational complexity, especially when the codeword length increases. A more tractable approach with limited space complexity was proposed in [5]. Nevertheless, the approach involves quantization, and thus the overall complexity depends not only on the codeword length but also on the required precision. On the other hand, a significantly simpler approach is Gaussian approximation (GA) [6]. Also initially developed for the design of LDPC codes, its applicability to polar code design has been well investigated [7]. It has been pointed out in [8] that GA with the original approximation function developed in [6] may not necessarily work accurately when the equivalent SNR values of the channels after polarization become low. Consequently, a modified version, which will be referred to as improved GA (IGA) in this work, has been proposed [8]. Furthermore, there have been various design approaches proposed in the recent literature, targeting specific polar decoding algorithms. For example, in the case of successive cancellation list (SCL) decoding [9] or belief propagation (BP) decoding [10], learning-based approaches such as genetic algorithms and reinforcement learning have been proposed in [11] and [12], respectively. The major limitations of these approaches are their lack of flexibility and scalability since computationally demanding training should be performed for each given combination of the code parameters such as block length and code rate.

In this work, we consider the application of the so-called *reciprocal channel approximation (RCA)*, introduced by Chung in [13], that is motivated by the duality property of mutual information that holds between a repetition code and parity-check code over a binary erasure channel (BEC) [14]. This approach has been originally adopted in the design of LDPC and other related codes [13, 15–18], and it was numerically demonstrated in [13, Chapter 7] that it offers a better approximation for density evolution in the case of BI-AWGN channels than the conventional GA. By numerical study and simulation, it will be shown that polar codes designed

based on RCA exhibit better performance than those based on (improved) GA, and the gain becomes noticeable as the block length increases. The superior performance improvement will be demonstrated for polar codes with very long lengths (such as $N = 2^{18}$ bits), as is considered in practical optical communications [19]. (See, also [20], where a polar code of length 2^{20} bits is considered.)

The design of polar codes based on RCA has been initially considered in [21] as well as [22]. RCA-based designs make use of the mutual information of BPSK signaling over an AWGN channel as well as its inverse function, which should be calculated numerically. There are several closed-form approximations available in the literature, and in [22] the two approximations developed in [16] and [23] are compared, indicating the sensitivity of polar code performance to the choice of approximation. For this reason, in this work we introduce rigorous closed-form expressions for the mutual information $C(\gamma)$ of BPSK as a function of SNR γ as well as its inverse function $C^{-1}(\cdot)$ that can be used for design of polar codes with long codeword lengths.

The main contributions of this work are as follows:

- We derive a closed-form piece-wise continuous mutual information expression for BPSK signaling over AWGN channels with guaranteed convergence in the case of high and low SNR based on the asymptotic analysis of the mutual information function. This expression is exploited to design polar codes based on RCA supporting a wide range of SNR after polarization.
- We develop an explicit algorithm that identifies SNR after channel polarization using only closed-form equations, which can thus be calculated with low complexity.
- By simulation, we demonstrate that the RCA-based design can achieve better performance as well as offer a better block error rate (BLER) estimate compared to GA-based approaches, especially as the block length increases and the code rate is moderate (e.g., around 1/2).

The remainder of the paper is organized as follows. Section II reviews the principle of RCA from the viewpoint of polar code design and develops a general algorithm. The key function $\Lambda(\xi)$ that corresponds to the *reciprocal channel mapping* defined in [13] and that transforms SNR in the log domain based on RCA, is introduced. Section III develops closed-form expressions of the mutual information for BPSK signaling as well as its inverse, and its accuracy is compared with two other formulas available in the literature. Based on the developed mathematical tools, closed-form approximations for the associated function $\Lambda(\xi)$ are derived in Section IV, which completes the proposed algorithm. Simulation results as well as the estimated BLER are compared in

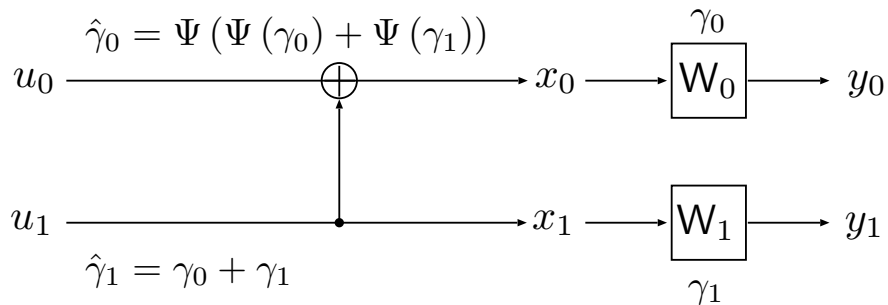


Fig. 1. Polar encoder and associated notations for $N = 2$.

Section V, which reveals the effectiveness of the RCA-based polar code design using the proposed algorithm. Finally, concluding remarks are given in Section VI.

II. POLAR CODES AND RECIPROCAL CHANNEL APPROXIMATION

A. Polar Codes

We start with the simplest binary polar code of codeword (or block) length $N = 2$ (Arıkan's kernel) shown in Fig. 1, where the information bits $u_0, u_1 \in \mathbb{F}_2$ and the coded bits $x_0, x_1 \in \mathbb{F}_2$ are related by

$$\begin{cases} x_0 &= u_0 + u_1, \\ x_1 &= u_1. \end{cases} \quad (1)$$

The coded bits x_0 and x_1 are modulated by BPSK and are transmitted over AWGN channels, denoted by W_0 and W_1 , where the SNRs of the channels are γ_0 and γ_1 , respectively, as illustrated in Fig. 1, with the received symbols given by y_0 and y_1 .

Assuming that u_0 is decoded first, since

$$u_0 = x_0 + x_1, \quad (2)$$

u_0 can be seen as a check node connected to x_0 and x_1 in the Tanner graph. Once the estimate of u_0 , denoted by $\hat{u}_0 \in \mathbb{F}_2$, is given, u_1 can be uniquely determined by either of x_0 or x_1 , i.e., u_1 is a variable node connected to both x_0 and x_1 .

Polar codes of length $N = 2^n$ for an integer $n > 1$ can be obtained by the recursive application of the above kernel [1].

B. RCA

Following [18], we briefly describe the principle of RCA. Let us first consider a BEC where the erasure probability is e^{-s} and the non-erasure probability e^{-r} , i.e., $e^{-s} + e^{-r} = 1$, for $s, r > 0$. Let $C(s)$ denote the capacity of this channel, i.e., $C(s) = 1 - e^{-s}$. Then, it follows that $C(s) + C(r) = 1$. Let s_i denote the above parameter s for the bit x_i transmitted over the corresponding BEC and let us define r_i such that $e^{-s_i} + e^{-r_i} = 1$. For a variable node u_1 connected to x_0 and x_1 , its erasure probability is given by $e^{-s_0}e^{-s_1} = e^{-(s_0+s_1)}$, i.e., it is characterized by the sum of s_0 and s_1 . For a check node u_0 connected to x_0 and x_1 , its corresponding *non-erasure* probability is given by $(1 - e^{-s_0})(1 - e^{-s_1}) = e^{-(r_0+r_1)}$, i.e., it is also characterized by the sum of r_0 and r_1 . In other words, for BEC, the parameter s is additive for variable nodes, whereas the parameter r is additive for check nodes [18].

We now apply the above RCA concept to the binary-input AWGN (BI-AWGN) channel. We define $C(\gamma)$ as the capacity of the BI-AWGN channel with the signal-to-noise power ratio (SNR) given by γ . Similar to BEC, the additive property holds for the parameter γ in the case of the variable node as long as all the connecting nodes are associated with mutually independent AWGN channels. This stems from the fact that the LLR is additive at the variable node, and both mean and variance of the LLR corresponding to BI-AWGN channels are proportional to the channel SNR [8]. Let us now define the SNR parameter λ corresponding to the check node such that $C(\gamma) + C(\lambda) = 1$, and assume that the additive property also holds for the parameter λ at the check node. Since this does not strictly hold for general BI-AWGN channels, this is an *approximation*, which is thus referred to as the reciprocal channel approximation (RCA) in [13, Section 7.4].

For a given channel SNR γ , the parameter λ can be found by solving

$$C(\lambda) = 1 - C(\gamma), \quad (3)$$

for λ . Since $C(\gamma)$ is a strictly increasing function for $\gamma > 0$, we can define its inverse function $C^{-1}(\cdot)$ and write

$$\lambda = C^{-1}(1 - C(\gamma)) \triangleq \Psi(\gamma). \quad (4)$$

The above function corresponds to the *reciprocal channel mapping* introduced in [13, Definition 7.3], also referred to as *self-inverting reciprocal energy function* in [18], applied to BI-AWGN channels. Our goal is to find a suitable expression for the function $\Psi(\gamma)$ that can support a wide

range of SNR value γ with high accuracy. Note that since (3) holds with λ and γ interchanged, one can easily verify that

$$\Psi(\Psi(\gamma)) = \gamma, \quad (5)$$

i.e., $\Psi(\gamma)$ is a self-inverse function satisfying $\Psi(\gamma) = \Psi^{-1}(\gamma)$ [13].

If γ_0 and γ_1 are the SNRs of the channels where the bits x_0 and x_1 are transmitted, respectively, then the SNR corresponding to the variable node u_1 , denoted by $\hat{\gamma}_1$, is expressed as

$$\hat{\gamma}_1 = \gamma_0 + \gamma_1. \quad (6)$$

On the other hand, the SNR corresponding to the check node u_0 , denoted by $\hat{\gamma}_0$, is similarly expressed based on the RCA principle [13, Section 7.4] as

$$\Psi(\hat{\gamma}_0) = \Psi(\gamma_0) + \Psi(\gamma_1), \quad (7)$$

from which we obtain

$$\hat{\gamma}_0 = \Psi^{-1}(\Psi(\gamma_0) + \Psi(\gamma_1)) = \Psi(\Psi(\gamma_0) + \Psi(\gamma_1)). \quad (8)$$

The above relationship between the pairs (γ_0, γ_1) and $(\hat{\gamma}_0, \hat{\gamma}_1)$ is illustrated in Fig. 1.

In what follows, we consider the case when γ is extremely large or small due to the polarization effect. From the viewpoint of numerical evaluation and similar to [8], it would be convenient to express γ in the log domain. Therefore, we define $\xi \triangleq \ln \gamma$ and also introduce the function

$$\Lambda(\xi) \triangleq \ln \Psi(e^\xi). \quad (9)$$

For the check node, the output $\hat{\xi}_0$ for a given pair of inputs $\xi_0 = \ln \gamma_0$ and $\xi_1 = \ln \gamma_1$ can be expressed as

$$\hat{\xi}_0 = \Lambda(\max(\Lambda(\xi_0), \Lambda(\xi_1)) + \ln(1 + e^{-|\Lambda(\xi_1) - \Lambda(\xi_0)|})). \quad (10)$$

On the other hand, for the variable node, the output $\hat{\xi}_1$ is expressed as

$$\hat{\xi}_1 = \max(\xi_0, \xi_1) + \ln(1 + e^{-|\xi_0 - \xi_1|}). \quad (11)$$

Algorithm 1 Channel Polarization with RCA (for Distinct Channel SNRs).

Input: $n = \log_2 N$, $\xi[0], \xi[1], \dots, \xi[N-1]$ as $\ln \gamma_0, \ln \gamma_1, \dots, \ln \gamma_{N-1}$.

Output: $\xi[0], \xi[1], \dots, \xi[N-1]$ as $\ln \hat{\gamma}_0, \ln \hat{\gamma}_1, \dots, \ln \hat{\gamma}_{N-1}$

```

1: for  $i = 1 : n$  do
2:    $J \leftarrow 2^i$ 
3:   for  $k = 0 : N/J - 1$  do
4:     for  $j = 0 : J/2 - 1$  do
5:        $\xi_0 \leftarrow \xi[kJ + j]$ 
6:        $\xi_1 \leftarrow \xi[kJ + j + J/2]$ 
7:        $\Lambda_0 \leftarrow \Lambda(\xi_0)$ 
8:        $\Lambda_1 \leftarrow \Lambda(\xi_1)$ 
9:        $\xi[kJ + j] \leftarrow \Lambda(\max(\Lambda_0, \Lambda_1) + \ln(1 + e^{-|\Lambda_0 - \Lambda_1|}))$ 
10:       $\xi[kJ + j + J/2] \leftarrow \max(\xi_0, \xi_1) + \ln(1 + e^{-|\xi_0 - \xi_1|})$ 
11:     end for
12:   end for
13: end for
14: return  $\xi[0], \xi[1], \dots, \xi[N-1]$ 

```

C. General Algorithm

In the case of a binary polar code of length $N = 2^n$, let $\gamma_0, \gamma_1, \dots, \gamma_{N-1}$ denote the channel SNRs of the coded bits x_0, x_1, \dots, x_{N-1} . Then the SNRs for the input bits u_0, u_1, \dots, u_{N-1} , denoted by $\hat{\gamma}_0, \hat{\gamma}_1, \dots, \hat{\gamma}_{N-1}$, can be obtained by the well-known recursive procedure in [1]. The corresponding RCA algorithm when each channel has a distinct SNR value is summarized in **Algorithm 1**. The algorithm can be significantly simplified when all the channels have the same SNR (or design SNR), i.e., $\gamma_0 = \gamma_1 = \dots = \gamma_{N-1}$, which is summarized in **Algorithm 2**.

The remaining questions are: how can one calculate the function $\Lambda(\xi)$ accurately with computational efficiency, i.e., without resorting to numerical integration, and how well does the algorithm operate compared to other known approaches of similar complexity? These will be addressed in the subsequent sections.

Algorithm 2 Channel Polarization with RCA (for Uniform Channel SNR).

Input: $n = \log_2 N$, $\xi[0] = \ln \gamma_0$

Output: $\xi[0], \xi[1], \dots, \xi[N-1]$ as $\ln \hat{\gamma}_0, \ln \hat{\gamma}_1, \dots, \ln \hat{\gamma}_{N-1}$

```

1: for  $i = 1 : n$  do
2:    $J \leftarrow 2^i$ 
3:   for  $j = 0 : J/2 - 1$  do
4:      $\xi_0 \leftarrow \xi[j]$ 
5:      $\Lambda_0 \leftarrow \Lambda(\xi_0)$ 
6:      $\xi[j] \leftarrow \Lambda(\Lambda_0 + \ln 2)$ 
7:      $\xi[j + J/2] \leftarrow \xi_0 + \ln 2$ 
8:   end for
9: end for
10: return  $\xi[0], \xi[1], \dots, \xi[N-1]$ 

```

III. CAPACITY EXPRESSION

A. Approximation for BI-AWGN Capacity

We start with the BI-AWGN capacity formula. Let E_s denote the symbol energy of BPSK and N_0 denote the variance of complex Gaussian noise. Let us define the SNR parameter γ as $\gamma \triangleq E_s/N_0$ in what follows. To compute the mutual information $C(\gamma)$ between a BPSK input and its corresponding output over an AWGN channel, the following equivalent J -function (see [16]) is often adopted:

$$J(x) = 1 - \frac{1}{\sqrt{2\pi x^2}} \int_{-\infty}^{\infty} e^{-\frac{(t-\frac{x^2}{2})^2}{2x^2}} \log_2(1 + e^{-t}) dt, \quad (12)$$

where x corresponds to the standard deviation of the LLR and thus is related to γ by $x = \sqrt{8\gamma}$. Then $C(\gamma) = J(\sqrt{8\gamma})$.

According to [16], the function $J(x)$ is well approximated numerically by

$$J(x) \approx \begin{cases} a_1 x^3 + b_1 x^2 + c_1 x, & 0 \leq x \leq 1.6363, \\ 1 - e^{a_2 x^3 + b_2 x^2 + c_2 x + d}, & 1.6363 < x \leq 10, \\ 1, & x > 10, \end{cases} \quad (13)$$

with

$$\begin{aligned} a_1 &= -0.0421061, \quad b_1 = 0.209252, \quad c_1 = -0.00640081, \\ a_2 &= 0.00181491, \quad b_2 = -0.142675, \quad c_2 = -0.0822054, \quad d = 0.0549608. \end{aligned}$$

On the other hand, in [23], the approximation

$$J(x) \approx \left(1 - 2^{-H_1 x^{2H_2}}\right)^{H_3}, \quad (14)$$

was proposed with $H_1 = 0.3073$, $H_2 = 0.8935$, and $H_3 = 1.1064$.

B. New Approximation Formula

From (12) and $C(\gamma) = J(\sqrt{8\gamma})$, we define

$$\begin{aligned} U(\gamma) &\triangleq 1 - C(\gamma) \\ &= \frac{1}{4\sqrt{\pi\gamma}} \int_{-\infty}^{\infty} e^{-\frac{1}{16\gamma}(t-4\gamma)^2} \log_2(1 + e^{-t}) dt. \end{aligned} \quad (15)$$

In what follows, we divide the range of γ , $\mathcal{R} \triangleq (0, \infty)$, into the four sub-regions $\mathcal{R}_1, \mathcal{R}_2, \mathcal{R}_3, \mathcal{R}_4$, where $\mathcal{R}_1 = (0, \Gamma_1)$, $\mathcal{R}_2 = [\Gamma_1, \Gamma_2)$, $\mathcal{R}_3 = [\Gamma_2, \Gamma_3)$, and $\mathcal{R}_4 = [\Gamma_3, \infty)$, with $\Gamma_1, \Gamma_2, \Gamma_3$ representing appropriate boundaries to be determined numerically.

1) *Low SNR Case:* For the sub-region \mathcal{R}_1 , i.e., when $\gamma \approx 0$, by Maclaurin series expansion we obtain

$$C(\gamma) \approx \frac{1}{\ln 2} \left(\gamma - \gamma^2 + \frac{4}{3}\gamma^3 - \frac{10}{3}\gamma^4 + \frac{208}{15}\gamma^5 \right). \quad (16)$$

By truncating up to the third order, we may approximate $U(\gamma)$ as

$$U_1(\gamma) \triangleq 1 - \frac{1}{\ln 2} \left(\gamma - \gamma^2 + \frac{4}{3}\gamma^3 \right), \quad \gamma < \Gamma_1. \quad (17)$$

By setting the upper boundary as $\Gamma_1 = 0.04$, the value of $U(\gamma)$ at $\gamma = \Gamma_1$ is calculated by numerical integration as

$$U(\Gamma_1) \approx 0.9444880, \quad (18)$$

whereas the corresponding approximation according to (17) is given by

$$U_1 \triangleq U_1(\Gamma_1) \approx 0.9444774. \quad (19)$$

Therefore, the approximation error of $U(\gamma)$ by $U_1(\gamma)$ in the region \mathcal{R}_1 is bounded by

$$|U(\gamma) - U_1(\gamma)| < 1.1 \times 10^{-5}, \quad \gamma < \Gamma_1. \quad (20)$$

2) *High SNR Case*: We next consider the sub-region \mathcal{R}_4 , i.e., when γ becomes larger than some boundary Γ_3 . By applying the series expansion of the exponential function $e^x = \sum_{k=0}^{\infty} \frac{x^k}{k!}$ to $U(\gamma)$ of (15), we obtain

$$\begin{aligned} U(\gamma) &= \frac{e^{-\gamma}}{4\sqrt{\pi\gamma}} \sum_{k=0}^{\infty} \frac{(-1)^k}{k! (16\gamma)^k} c_k \\ &= \frac{e^{-\gamma}}{4\sqrt{\pi\gamma}} \left\{ c_0 - \frac{c_1}{16\gamma} + \frac{c_2}{2 \cdot (16\gamma)^2} - \dots \right\}, \end{aligned} \quad (21)$$

where

$$c_k \triangleq \int_{-\infty}^{\infty} e^{\frac{t}{2}} t^{2k} \log_2(1 + e^{-t}) dt. \quad (22)$$

The above expression agrees with [3, Problem 4.12]. Note that c_k for specific values of k can be expressed in closed form, e.g.,

$$c_0 = \frac{2\pi}{\ln 2}, \quad c_1 = \frac{2\pi(8 + \pi^2)}{\ln 2}, \quad c_2 = \frac{2\pi(384 + 48\pi^2 + 5\pi^4)}{\ln 2}. \quad (23)$$

Although the approximation becomes tighter as we incorporate more terms in (21), it becomes infeasible to find the corresponding inverse expression in closed form. Therefore, we adopt the expression

$$U_4(\gamma) \triangleq \alpha \frac{e^{-\gamma}}{\sqrt{\gamma}}, \quad \gamma > \Gamma_3, \quad (24)$$

where α and Γ_3 are appropriate constants to be determined. By setting the boundary as $\Gamma_3 = 10$, the value at the boundary becomes

$$U_3 \triangleq U(\Gamma_3) \approx 1.667 \times 10^{-5}, \quad (25)$$

from which we fix the constant α as

$$\alpha \approx 1.16125142, \quad (26)$$

such that $U(\Gamma_3) \approx U_4(\Gamma_3)$. Note that this is different from the exact coefficient of the first term in (21), which is given by

$$\alpha_0 \triangleq c_0/(4\sqrt{\pi}) = \frac{\sqrt{\pi}}{2(\ln 2)} \approx 1.27856, \quad (27)$$

and thus the exact asymptotic form for large γ would be

$$U(\gamma) \rightarrow \frac{\sqrt{\pi}}{2(\ln 2)} \frac{e^{-\gamma}}{\sqrt{\gamma}}, \quad (28)$$

as discussed in [3, 24]. As γ increases, the use of α_0 may become more accurate eventually, but for our purpose, the use of (26) may be more suitable as the piece-wise continuity of the approximate function can be guaranteed.

3) *Moderate SNR Case:* We first note that the main advantage of the capacity approximation form (14) is that its inverse function can also be expressed in closed form. We thus adopt this form for the remaining sub-regions \mathcal{R}_2 and \mathcal{R}_3 and define the functions for the two adjacent regions as

$$U_2(\gamma) \triangleq 1 - \left(1 - e^{-H_{2,1}\gamma^{H_{2,2}}}\right)^{H_{2,3}}, \quad \Gamma_1 < \gamma < \Gamma_2, \quad (29)$$

$$U_3(\gamma) \triangleq 1 - \left(1 - e^{-H_{3,1}\gamma^{H_{3,2}}}\right)^{H_{3,3}}, \quad \Gamma_2 < \gamma < \Gamma_3, \quad (30)$$

where the constants $H_{i,j}$ for $i \in \{2, 3\}$ and $j \in \{1, 2, 3\}$ should be determined appropriately depending on the boundary Γ_2 . In what follows, we fix the boundary as $\Gamma_2 = 1$ for simplicity of numerical evaluation. Then the precise value of $U(\gamma)$ at the boundary is obtained by numerical integration as

$$U_2 \triangleq U(\Gamma_2) \approx 0.2785484. \quad (31)$$

Furthermore, in order to guarantee the piece-wise continuity of the approximate function for $U(\gamma)$, it is required that

$$U_2(\Gamma_1) = U_1, \quad U_3(\Gamma_3) = U_3. \quad (32)$$

Let us first consider the function $U_2(\gamma)$. By the relationships at the boundaries, one may express

$$H_{2,1} = -\ln \left(1 - (1 - U_2)^{\frac{1}{H_{2,3}}}\right), \quad (33)$$

$$H_{2,2} = \left[\ln \left(\frac{\Gamma_2}{\Gamma_1}\right)\right]^{-1} \ln \left\{ \frac{\ln \left(1 - (1 - U_2)^{\frac{1}{H_{2,3}}}\right)}{\ln \left(1 - (1 - U_1)^{\frac{1}{H_{2,3}}}\right)} \right\}. \quad (34)$$

As a consequence, $U_2(\gamma)$ can be expressed as a function of γ and $H_{2,3}$, which we explicitly write as $U_2(\gamma; H_{2,3})$. Based on the minimization of ∞ -norm, we may optimize the coefficients $H_{2,3}$ as

$$H_{2,3} = \arg \min_H \max_{\Gamma_1 < \gamma < \Gamma_2} |U_2(\gamma; H) - U(\gamma)|, \quad (35)$$

based on which we numerically obtain

$$H_{2,1} = 1.396634, \quad H_{2,2} = 0.872764, \quad H_{2,3} = 1.148562.$$

Likewise, by denoting $U_3(\gamma)$ as a function of $H_{3,3}$, i.e., $U_3(\gamma; H_{3,3})$, since

$$H_{3,1} = -\ln \left(1 - (1 - U_2)^{\frac{1}{H_{3,3}}} \right), \quad (36)$$

$$H_{3,2} = \left[\ln \left(\frac{\Gamma_3}{\Gamma_2} \right) \right]^{-1} \ln \left\{ \frac{\ln \left(1 - (1 - U_3)^{\frac{1}{H_{3,3}}} \right)}{\ln \left(1 - (1 - U_2)^{\frac{1}{H_{3,3}}} \right)} \right\}, \quad (37)$$

one may determine $H_{3,3}$ according to

$$H_{3,3} = \arg \min_H \max_{\Gamma_2 < \gamma < \Gamma_3} |U_3(\gamma; H) - U(\gamma)|, \quad (38)$$

and thus numerically obtain

$$H_{3,1} = 1.266967, \quad H_{3,2} = 0.938175, \quad H_{3,3} = 0.986830.$$

4) *Summary:* We summarize the closed-form piece-wise continuous approximate function $\hat{U}(\gamma)$ for $U(\gamma)$:

$$\hat{U}(\gamma) = \begin{cases} U_1(\gamma) = 1 - \frac{1}{\ln 2} (\gamma - \gamma^2 + \frac{4}{3}\gamma^3), & \gamma < \Gamma_1, \\ U_2(\gamma) = 1 - \left(1 - e^{-H_{2,1}\gamma^{H_{2,2}}} \right)^{H_{2,3}}, & \Gamma_1 \leq \gamma < \Gamma_2, \\ U_3(\gamma) = 1 - \left(1 - e^{-H_{3,1}\gamma^{H_{3,2}}} \right)^{H_{3,3}}, & \Gamma_2 \leq \gamma < \Gamma_3, \\ U_4(\gamma) = \alpha \frac{e^{-\gamma}}{\sqrt{\gamma}}, & \gamma \geq \Gamma_3, \end{cases} \quad (39)$$

where $\Gamma_1 = 0.04, \Gamma_2 = 1, \Gamma_3 = 10$. As a consequence, the approximate formula of the capacity for the BI-AWGN channel, $\hat{C}(\gamma) \triangleq 1 - \hat{U}(\gamma)$, can be summarized as

$$\hat{C}(\gamma) = \begin{cases} \frac{1}{\ln 2} (\gamma - \gamma^2 + \frac{4}{3}\gamma^3), & \gamma \in \mathcal{R}_1, \\ \left(1 - e^{-H_{2,1}\gamma^{H_{2,2}}} \right)^{H_{2,3}}, & \gamma \in \mathcal{R}_2, \\ \left(1 - e^{-H_{3,1}\gamma^{H_{3,2}}} \right)^{H_{3,3}}, & \gamma \in \mathcal{R}_3, \\ 1 - \alpha \frac{e^{-\gamma}}{\sqrt{\gamma}}, & \gamma \in \mathcal{R}_4. \end{cases} \quad (40)$$

C. Numerical Results

To investigate the accuracy of the developed approximation, we define the error function as

$$\epsilon(\gamma) \triangleq U(\gamma) - \hat{U}(\gamma) = \hat{C}(\gamma) - C(\gamma). \quad (41)$$

We calculate $C(\gamma)$ based on the numerical integration and compare with the developed expression as well as (13) of [16] and (14) of [23]. In Fig. 2, we plot the absolute value of the error function

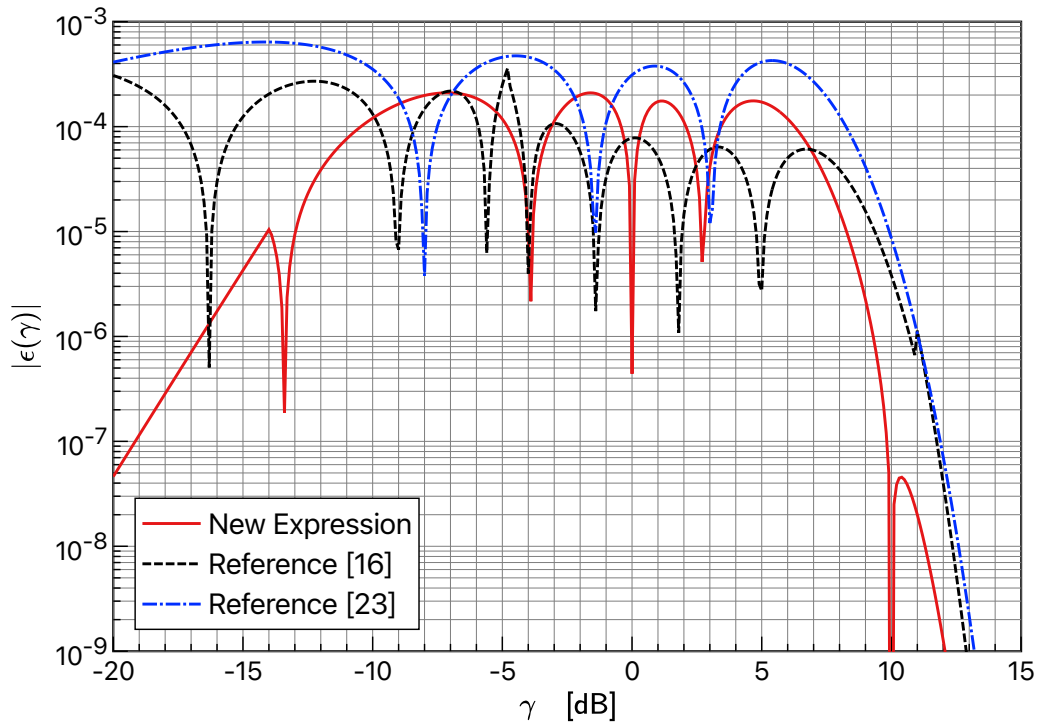


Fig. 2. Approximation error of the proposed expression. Those based on ten Brink *et al.* [16] and Brännström *et al.* [23] are also shown for comparison.

$\epsilon(\gamma)$ with respect to γ in dB. We observe that the absolute values of the approximation error for all the three expressions are less than 10^{-3} , and monotonically decrease for higher and lower SNR regions. Nevertheless, the most significant difference of the proposed expression is that the error becomes much less than 10^{-5} as SNR decreases since we selected the associated parameters such that the condition (20) holds. Also, since the proposed expression $\hat{C}(\gamma)$ in (40) is designed to be piece-wise continuous with respect to γ , we also observe that the error function is piece-wise continuous as well. By comparison, as observed in Fig. 2, the approximation based on (13) (introduced in [16]) exhibits discontinuities at the boundaries corresponding to $x = 1.6363$ and $x = 10$, i.e., $\gamma = -4.7536$ dB and $\gamma = 10.969$ dB, respectively.

IV. DERIVATION OF CLOSED-FORM EXPRESSION FOR $\Lambda(\xi)$

Our next step is to find a suitable approximate expression for $\Lambda(\xi)$ introduced in (9). We first consider an approximation for its constituent function $\Psi(\gamma)$. From (4), we have

$$\Psi(\gamma) = C^{-1}(1 - C(\gamma)) = C^{-1}(U(\gamma)). \quad (42)$$

Therefore, it is necessary to find the inverse function for $\hat{C}(\gamma)$ defined in (40).

Let us first consider the case $\gamma \in \mathcal{R}_1$. From (40), the inverse function for the equation $\hat{C}(\gamma) = c$ can be expressed as

$$\hat{C}^{-1}(c) = \frac{1}{4} \left(1 - \frac{3}{A(c)} + A(c) \right), \quad c < C_1, \quad (43)$$

where $C_1 \triangleq 1 - U_1$ and

$$A(c) \triangleq \left(-5 + 24(\ln 2)c + 2\sqrt{13 + 12(\ln 2)c(12(\ln 2)c - 5)} \right)^{\frac{1}{3}}. \quad (44)$$

On the other hand, when $\gamma \in \mathcal{R}_2$, we have

$$\hat{C}^{-1}(c) = \left[-\frac{1}{H_{2,1}} \ln \left(1 - I^{\frac{1}{H_{2,3}}} \right) \right]^{\frac{1}{H_{2,2}}}, \quad C_1 < c < C_2, \quad (45)$$

where $C_2 = 1 - U_2$. The function $\hat{C}^{-1}(c)$ in the case of $\gamma \in \mathcal{R}_3$ can be derived in a similar manner. Finally, in the case of $\gamma \in \mathcal{R}_4$, we have

$$\hat{C}^{-1}(c) = \frac{1}{2} W_0 \left(2 \left(\frac{\alpha}{1-c} \right)^2 \right), \quad c > C_3, \quad (46)$$

where $C_3 = 1 - U_3$ and $W_0(x)$ is the corresponding Lambert W function [25], i.e., the value of w that satisfies $we^w = x$ for a given $x > 0$.

In summary, we have

$$\hat{C}^{-1}(c) = \begin{cases} \frac{1}{4} \left(1 - \frac{3}{A(c)} + A(c) \right), & c < C_1 \approx 0.055523, \\ \left[-\frac{1}{H_{2,1}} \ln \left(1 - c^{\frac{1}{H_{2,3}}} \right) \right]^{\frac{1}{H_{2,2}}}, & C_1 \leq c < C_2 \approx 0.721452, \\ \left[-\frac{1}{H_{3,1}} \ln \left(1 - c^{\frac{1}{H_{3,3}}} \right) \right]^{\frac{1}{H_{3,2}}}, & C_2 \leq c < C_3 \approx 0.999983, \\ \frac{1}{2} W_0 \left(2 \left(\frac{\alpha}{1-c} \right)^2 \right), & c \geq C_3. \end{cases} \quad (47)$$

By substituting $\hat{U}(\gamma)$ of (39) into c of (47), we obtain the approximate value of $\Psi(\gamma) = C^{-1}(U(\gamma))$ for a given γ , which we denote by $\hat{\Psi}(\gamma) \triangleq \hat{C}^{-1}(\hat{U}(\gamma))$.

In what follows, we derive simple asymptotic closed-form expressions of $\hat{\Psi}(\gamma)$ and thus $\Lambda(\xi)$ when γ becomes extremely small or large in order to simplify the computation with negligible loss of accuracy. Also, as we will see, it is not actually necessary to implement the $W_0(\cdot)$ function for polar code construction.

A. For Small γ

We consider the case where γ is small and satisfies $\gamma \leq \Gamma_0$ for some boundary Γ_0 such that the condition $c = \hat{U}(\gamma) \geq C_3$ holds in (47). Then, it follows from (39) that

$$\hat{\Psi}(\gamma) = \frac{1}{2}W_0 \left(2 \left(\frac{\alpha}{\frac{1}{\ln 2} (\gamma - \gamma^2 + \frac{4}{3}\gamma^3)} \right)^2 \right), \quad \gamma < \min(\Gamma_0, \Gamma_1), \quad (48)$$

where Γ_0 corresponds to the value of γ that satisfies $\hat{U}(\gamma) = C_3$. By numerically solving the equation

$$\frac{1}{\ln 2} \left(\Gamma_0 - \Gamma_0^2 + \frac{4}{3}\Gamma_0^3 \right) = U_3, \quad (49)$$

with respect to Γ_0 , we obtain

$$\Gamma_0 \approx 1.21974 \times 10^{-5}, \quad (50)$$

and thus we observe that $\Gamma_0 \ll \Gamma_1$. By defining $f(\gamma) \triangleq \gamma - \gamma^2 + \frac{4}{3}\gamma^3$, we may express (48) as

$$\hat{\Psi}(\gamma) = \frac{1}{2}W_0 \left(2\alpha^2 (\ln 2)^2 f^{-2}(\gamma) \right), \quad \gamma < \Gamma_0. \quad (51)$$

Since the argument of the function $W_0(\cdot)$ in (51) becomes larger as γ decreases, we may invoke the following asymptotic form of $W_0(x)$ for large x [25]:

$$W_0(x) \approx \ln x - \ln \ln x + \frac{\ln \ln x}{\ln x} + \dots. \quad (52)$$

On applying (52) to (51), we note that

$$\ln \left(2\alpha^2 (\ln 2)^2 f^{-2}(\gamma) \right) = \ln 2 + 2 \ln(\ln 2) + 2 \ln \alpha - 2 \ln \gamma - 2 \ln \left(1 - \gamma + \frac{4}{3}\gamma^2 \right), \quad (53)$$

where the last term in the right hand side turns out to be negligible in the range of $\gamma < \Gamma_0$.

Thus, by defining the dominant terms as

$$B(\xi) \triangleq \ln 2 + 2 (\ln \alpha + \ln (\ln 2)) - 2\xi, \quad (54)$$

where $\xi \triangleq \ln \gamma$, we may equivalently express $\ln \hat{\Psi}(\gamma)$ with respect to ξ , denoted by $\Lambda(\xi)$, as

$$\Lambda(\xi) \approx \ln \left(B(\xi) + \left(\frac{1}{B(\xi)} - 1 \right) \ln B(\xi) \right) - \ln 2. \quad (55)$$

The above approximation is valid in the range of $\gamma < \Gamma_0$, i.e.,

$$\xi < \Xi_0 \triangleq \ln \Gamma_0 \approx -11.3143. \quad (56)$$

B. For Large γ

When $\gamma \geq \Gamma_3$, i.e., $\gamma \in \mathcal{R}_4$, we observe from (39) with (32) that $\hat{U}(\gamma) \leq U_3$ and thus

$$\hat{\Psi}(\gamma) = \frac{1}{4} \left(1 - \frac{3}{A(c)} + A(c) \right), \quad c = \alpha \frac{e^{-\gamma}}{\sqrt{\gamma}}. \quad (57)$$

For $A(c)$ in (44) with small c , since

$$\sqrt{13 + 12(\ln 2)c(12(\ln 2)c - 5)} \approx \sqrt{13} - \frac{30}{\sqrt{13}}(\ln 2)c, \quad (58)$$

we have

$$A(c) \approx \left(-5 + 2\sqrt{13} \right)^{\frac{1}{3}} \left(1 + \frac{4}{\sqrt{13}}(\ln 2)c \right), \quad (59)$$

and by substituting (59) into (57), we obtain

$$\hat{\Psi}(\gamma) \approx (\ln 2)c \left(1 - 2 \frac{\sqrt{13} + 1}{13 + 4\sqrt{13}(\ln 2)c} (\ln 2)c \right). \quad (60)$$

Taking the logarithm of both sides, we have

$$\ln \hat{\Psi}(\gamma) \approx \ln c + \ln(\ln 2) + \ln \left(1 - 2 \frac{\sqrt{13} + 1}{13 + 4\sqrt{13}(\ln 2)c} (\ln 2)c \right). \quad (61)$$

By substituting $c = \alpha \frac{e^{-\gamma}}{\sqrt{\gamma}}$ and noticing that the third term in the right-hand side of (61) becomes negligible as γ increases, we have

$$\ln \hat{\Psi}(\gamma) \approx \ln \alpha + \ln(\ln 2) - \gamma - \frac{1}{2} \ln \gamma, \quad (62)$$

or in terms of ξ as

$$\Lambda(\xi) \approx \ln \alpha + \ln(\ln 2) - e^\xi - \frac{1}{2}\xi. \quad (63)$$

Note that (62) indicates that $\hat{\Psi}(\gamma)$ becomes infinitesimal as γ increases.

C. Complete RCA Algorithm

In the previous section, the RCA algorithm was summarized as **Algorithm 1** and **Algorithm 2**, depending on the condition of the channel SNR. Based on the mathematical derivations in this section, the calculation process of the function $\Lambda(\xi)$ is summarized as **Algorithm 3**. Note that the complexity of GA-based approaches generally involves the use of an inverse function that cannot be described (or accurately approximated) using a closed form expression, and thus should be performed by resorting to some iterative algorithms (such as the bisection method). On the other hand, the proposed approach does not require such numerical algorithms and thus computational effort is in general lower than those based on GA (or IGA).

Algorithm 3 Calculating $\Lambda(\xi)$

Input: $\xi = \ln \gamma$
Output: $\Lambda(\xi) = \ln \Psi(\gamma)$

- 1: $\alpha = 1.16125, \Gamma_1 = 0.04, \Gamma_2 = 1, \Gamma_3 = 10, \Xi_0 = -11.3143$
 - 2: $C_1 = 0.055523, C_2 = 0.721452$
 - 3: $H_{2,1} = 1.396634, H_{2,2} = 0.872764, H_{2,3} = 1.148562$
 - 4: $H_{3,1} = 1.266967, H_{3,2} = 0.938175, H_{3,3} = 0.986830$
 - 5: **if** $\xi < \Xi_0$ **then**
 - 6: $B = \ln 2 + 2 \ln(\ln 2) + 2 \ln \alpha - 2\xi$
 - 7: **return** $\ln \left(B + \left(\frac{1}{B} - 1 \right) \ln B \right) - \ln 2$
 - 8: **end if**
 - 9: $\gamma \leftarrow \exp(\xi)$
 - 10: **if** $\gamma > \Gamma_3$ **then**
 - 11: **return** $\ln(\ln 2) + \ln \alpha - \gamma - \xi/2$
 - 12: **else if** $\gamma < \Gamma_1$ **then**
 - 13: $U \leftarrow 1 - \frac{1}{\ln 2}(\gamma - \gamma^2 + \frac{4}{3}\gamma^3)$
 - 14: **else if** $\gamma < \Gamma_2$ **then**
 - 15: $U \leftarrow 1 - \left(1 - e^{-H_{2,1}\gamma^{H_{2,2}}} \right)^{H_{2,3}}$
 - 16: **else**
 - 17: $U \leftarrow 1 - \left(1 - e^{-H_{3,1}\gamma^{H_{3,2}}} \right)^{H_{3,3}}$
 - 18: **end if**
 - 19: **if** $U < C_1$ **then**
 - 20: $A = \left(-5 + 24(\ln 2)U + 2\sqrt{13 + 12(\ln 2)U(12(\ln 2)U - 5)} \right)^{\frac{1}{3}}$
 - 21: **return** $\ln \left(1 - \frac{3}{A} + A \right) - 2 \ln 2$
 - 22: **else if** $U < C_2$ **then**
 - 23: **return** $\frac{1}{H_{2,2}} \left[\ln \left(-\ln \left(1 - U^{\frac{1}{H_{2,3}}} \right) \right) - \ln H_{2,1} \right]$
 - 24: **else**
 - 25: **return** $\frac{1}{H_{3,2}} \left[\ln \left(-\ln \left(1 - U^{\frac{1}{H_{3,3}}} \right) \right) - \ln H_{3,1} \right]$
 - 26: **end if**
-

V. SIMULATION RESULTS

In this section, we focus on the AWGN channels with BPSK, where the SNRs of all the channels are identical and given by $\gamma_0 = E_s/N_0$. We estimate the SNRs of the polarized channels $\hat{\gamma}_0, \hat{\gamma}_1, \dots, \hat{\gamma}_{N-1}$ by applying **Algorithm 2** in Section II. Let us sort $\hat{\gamma}_k$ such that

$$\hat{\gamma}_{I_0(\gamma_0)} \geq \hat{\gamma}_{I_1(\gamma_0)} \geq \dots \geq \hat{\gamma}_{I_{N-1}(\gamma_0)}, \quad (64)$$

where the subscript $I_k(\gamma_0)$ corresponds to the index of the input bit having the k th highest SNR (with $k = 0$ representing the maximum), with emphasis on the fact that the channel SNR is γ_0 . Let us define the index set $\mathcal{I}_K(\gamma_0)$ consisting of the K elements with highest SNRs as

$$\mathcal{I}_K(\gamma_0) \triangleq \{I_0(\gamma_0), I_1(\gamma_0), \dots, I_{K-1}(\gamma_0)\}, \quad (65)$$

where $R \triangleq K/N$ corresponds to the code rate.

Similar to the case of GA, we assume that the distribution of the LLR corresponding to the k th input bit is modeled as Gaussian with SNR $\hat{\gamma}_k$. Then, under the assumption that all the previous bits in the SC decoding are correctly decoded, the error rate of the k th bit can be estimated as

$$P_{b,k} = Q\left(\sqrt{\frac{\hat{\gamma}_k}{2}}\right), \quad (66)$$

with the Q -function defined as $Q(x) = \frac{1}{2}\text{erfc}\left(\frac{x}{\sqrt{2}}\right) = \frac{1}{\sqrt{2\pi}} \int_x^\infty e^{-\frac{t^2}{2}} dt$. The resulting *minimum estimated BLER* can be defined as [8]

$$P_{\text{BL}}(K, \gamma_0) \triangleq 1 - \prod_{k \in \mathcal{I}_K(\gamma_0)} \left(1 - Q\left(\sqrt{\frac{\hat{\gamma}_k}{2}}\right)\right). \quad (67)$$

Note that the above expression is a function of $\mathcal{I}_K(\gamma_0)$ only, i.e., the K largest estimated SNRs uniquely determines the BLER. Therefore, if the code rate R is low (i.e., the number of K is small) and estimation accuracy is good for low SNR region, the estimated BLER of (67) should become tight compared to the true BLER, which may be estimated by time-consuming simulations with a sufficiently large number of trials.

A. Comparison for Short Polar Codes

We first compare the minimum estimated BLER based on (67) calculated for the conventional GA, IGA of [8], and the proposed RCA as well as the corresponding simulation results in the cases of $N = 64$ and 1024 with three different code rates ($R = 0.25, 0.5, 0.75$). The results are listed in Table I. Note that the channel SNR (or design SNR) γ_0 is selected such that the

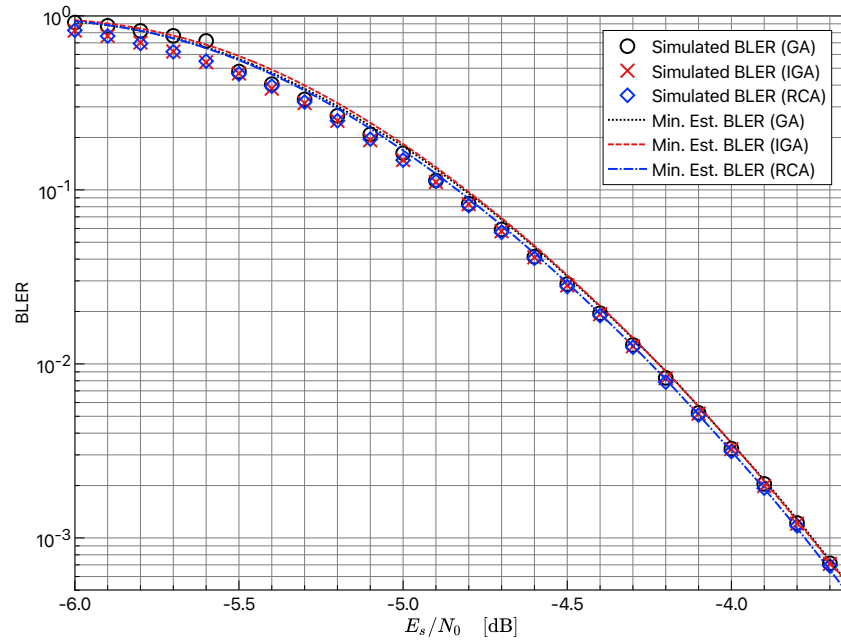
TABLE I
COMPARISON OF ESTIMATED BLER AND SIMULATION.

N	R	γ_0 [dB]	BLER (RCA)		BLER (IGA)		BLER (GA)	
			Estimate	Simulation	Estimate	Simulation	Estimate	Simulation
64	0.25	-2.53	0.0100	= IGA	0.0100	0.0095	0.0101	= IGA
	0.5	0.65	0.0100	= IGA	0.0100	0.0096	0.0102	= IGA
	0.75	3.26	0.0101	= IGA	0.0100	0.0099	0.0103	= IGA
1024	0.25	-3.97	0.0103	0.0100	0.0111	0.0102	0.0113	= IGA
	0.5	-0.50	0.0102	0.0103	0.0106	0.0104	0.0109	= IGA
	0.75	2.33	0.0104	= IGA	0.0102	0.0111	0.0109	= IGA

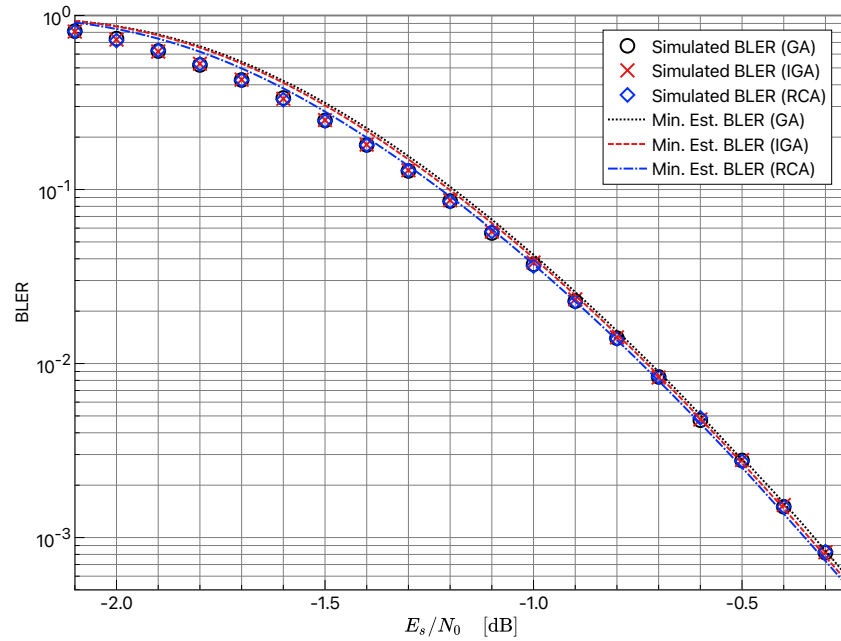
resulting BLER reaches around 10^{-2} , and the same value of γ_0 is applied for all three cases. Also, if the same polar code as IGA is constructed by any of the other schemes, this is indicated in the table. In such a case, the resulting code is the same and thus the simulation result for the BLER should be identical to that reported in the IGA column.

Analogous to the observation in [13, Chap. 7.4.1], the performances are similar for all the cases evaluated here. Note that the polar codes constructed by the three different schemes are identical in the case of $N = 64$. With a length of $N = 1024$ and for the cases of $R = 0.25$ and 0.5 , the codes constructed by RCA and IGA differ by only one bit position, and the corresponding simulation results indicate that the code designed by RCA very slightly outperforms that of IGA, whereas all the codes designed by the conventional GA are the same as those by IGA even in this case.

The BLER performances of these three approaches with $N = 2048$ bits are compared in Fig. 3 for code rates of $R = 0.25$ and $R = 0.5$. Note that for all the simulation results, the polar code is constructed *for each given channel SNR*. We observe that in the case of low code rate ($R = 0.25$) and low SNR region ($E_s/N_0 < -5.5$ dB), the performance degradation of GA compared to IGA and RCA is noticeable, as the approximation error of the conventional GA becomes significant with decreasing SNR as discussed in [8]. On the whole, however, the performance difference is almost negligible similar to those reported in Table I, justifying the effectiveness of the conventional GA as well as IGA for the polar codes with modest codeword lengths. Nevertheless, it is worth mentioning that the simulation results match best with the minimum estimated BLER calculated by the proposed RCA algorithm.



(a)



(b)

Fig. 3. Simulated BLER of the polar codes with $N = 2^{11}$ designed at each channel SNR as well as the minimum estimated BLER: (a) $R = 0.25$, (b) $R = 0.5$.

B. Comparison for Long Polar Codes

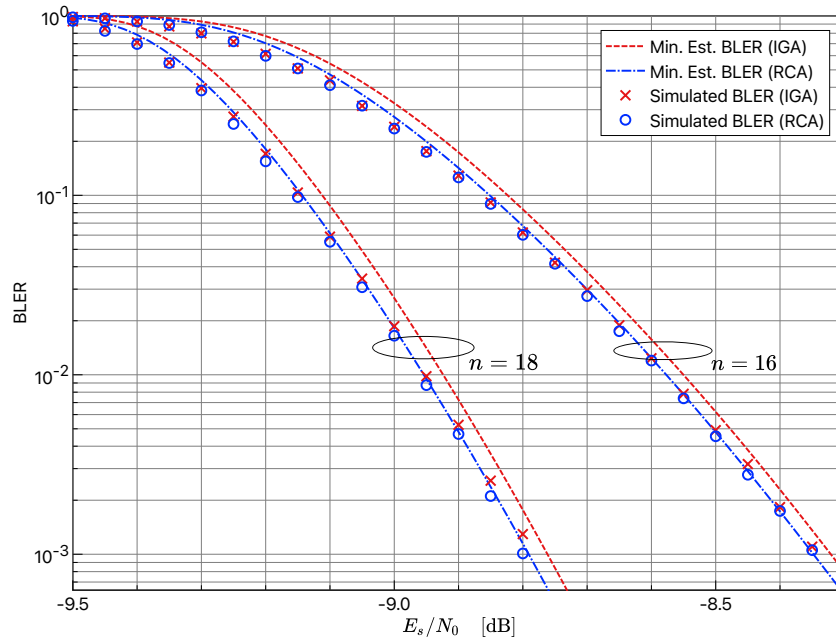
We now focus on the polar code performance with long block lengths ($N = 2^{16}$ and 2^{18}). Note that the performance of the conventional GA is not shown in the remaining figures as it becomes significantly worse than that of IGA as demonstrated in [8]. The cases with lower code rates ($R = 1/8$ and $R = 1/4$) are compared in Fig. 4, whereas those with higher code rates ($R = 1/2$ and $R = 3/4$) are shown in Fig. 5. We observe that for all the cases compared, the polar codes designed based on the proposed RCA algorithms outperform those based on IGA, and the gap is especially noticeable when the code rate is low. We also notice that, similar to the results in Fig. 3, the minimum estimated BLER values computed from (67) and those obtained by simulation are in general closer when RCA is employed, indicating that the estimation accuracy of the equivalent SNR obtained by RCA is higher than that of IGA. Therefore, considering the fact that the computational complexity required for performing GA, IGA, and RCA is almost the same, the proposed RCA may be preferable to GA-based approaches, especially when polar codes with long block lengths and moderate code rates should be designed under severe limitation of computational resources.

VI. CONCLUSIONS

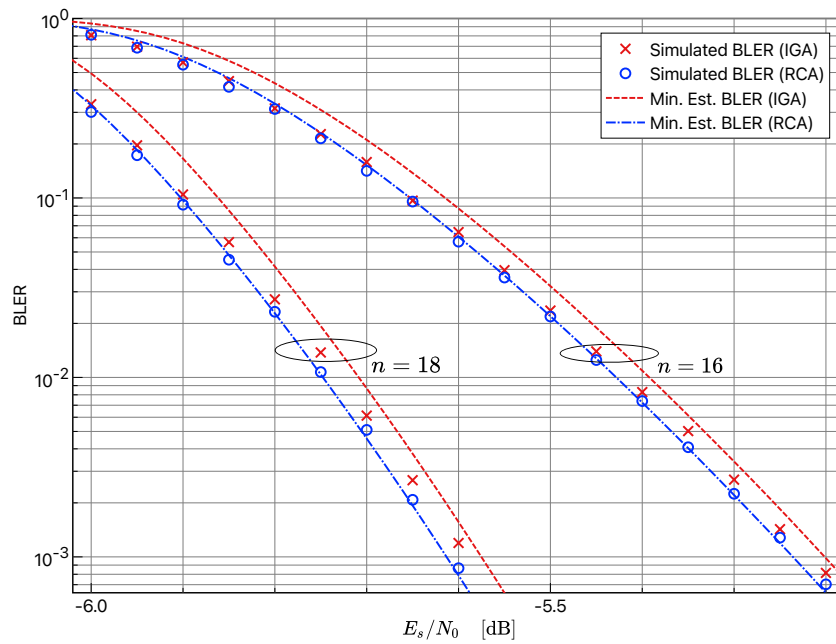
In this work, we have proposed an explicit closed-form algorithm for polar code design based on RCA. Simulation results have shown that polar code designed based on the proposed RCA can outperform popular Gaussian approximation (GA)-based approaches with no increase of computational complexity. Moreover, the estimated BLER performances from RCA are closer to those obtained by simulation compared to those based on GA, indicating the accuracy of RCA compared to GA. The benefit of the proposed approach becomes significant for polar codes with large block lengths and moderate code rates.

REFERENCES

- [1] E. Arıkan, "Channel polarization: A method for constructing capacity-achieving codes for symmetric binary-input memoryless channels," *IEEE Trans. Inform. Theory*, vol. 55, pp. 3051–3073, 2009.
- [2] T. J. Richardson, M. A. Shokrollahi, and R. L. Urbanke, "Design of capacity-approaching irregular low-density parity-check codes," *IEEE Trans. Inform. Theory*, vol. 47, pp. 619–637, Feb. 2001.
- [3] T. J. Richardson and R. L. Urbanke, *Modern Coding Theory*. Cambridge; New York: Cambridge University Press, 2008.
- [4] R. Mori and T. Tanaka, "Performance of polar codes with the construction using density evolution," *IEEE Commun. Lett.*, vol. 13, pp. 519–521, July 2009.

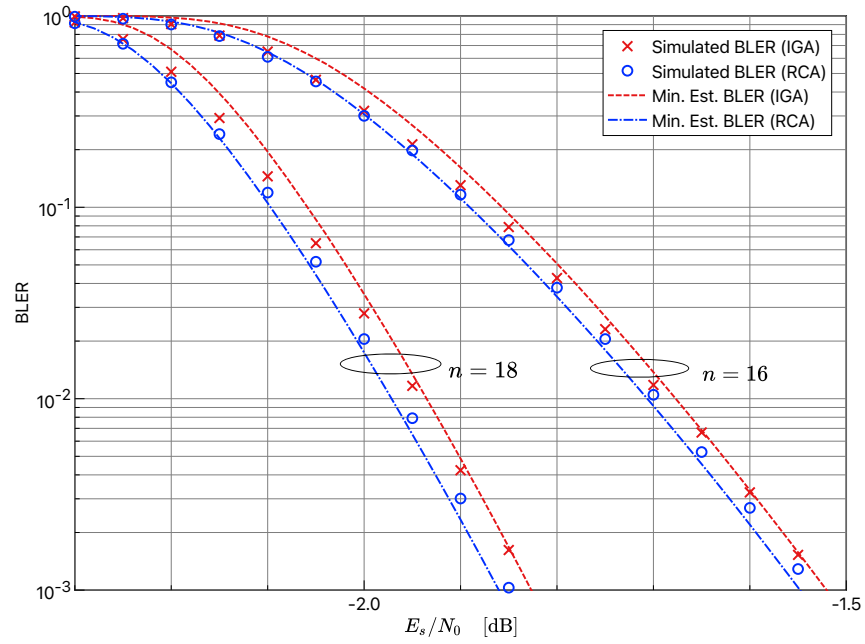


(a)

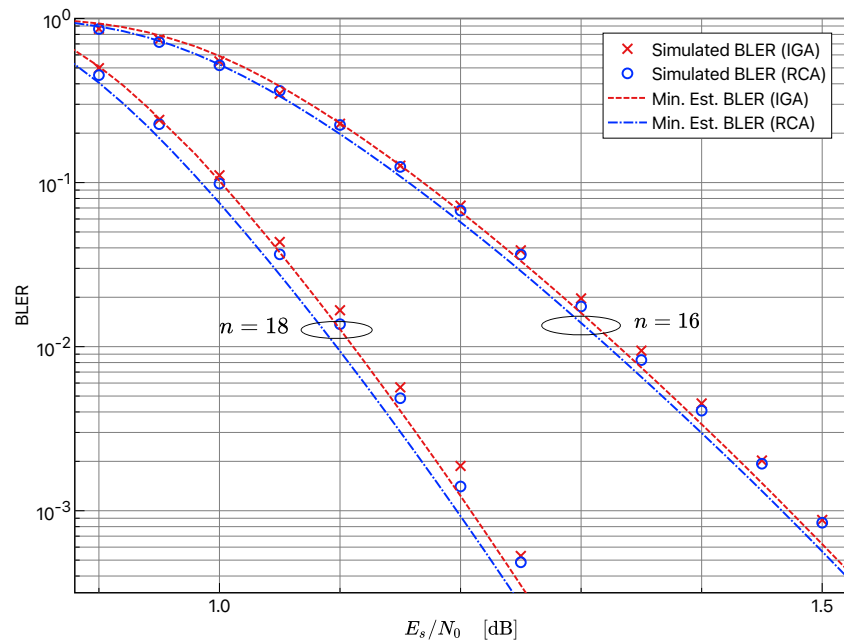


(b)

Fig. 4. Simulated BLER of the long polar codes with $N = 2^n$ ($n = 16$ and 18) designed at each channel SNR as well as the minimum estimated BLER: (a) $R = 0.125$, (b) $R = 0.25$.



(a)



(b)

Fig. 5. Simulated BLER of the long polar codes with $N = 2^n$ ($n = 16$ and 18) designed at each channel SNR as well as the minimum estimated BLER: (a) $R = 0.5$, (b) $R = 0.75$.

- [5] I. Tal and A. Vardy, “How to construct polar codes,” *IEEE Trans. Inform. Theory*, vol. 59, pp. 6562–6582, Oct. 2013.
- [6] S.-Y. Chung, T. Richardson, and R. Urbanke, “Analysis of sum-product decoding of low-density parity-check codes using a Gaussian approximation,” *IEEE Trans. Inform. Theory*, vol. 47, pp. 657–670, Feb. 2001.
- [7] P. Trifonov, “Efficient design and decoding of polar codes,” *IEEE Trans. Commun.*, vol. 60, pp. 3221–3227, Nov. 2012.
- [8] H. Ochiai, P. Mitran, and H. V. Poor, “Capacity-approaching polar codes with long codewords and successive cancellation decoding based on improved Gaussian approximation,” *IEEE Trans. Commun.*, vol. 69, pp. 31–43, Jan. 2021.
- [9] I. Tal and A. Vardy, “List decoding of polar codes,” *IEEE Trans. Inform. Theory*, vol. 61, pp. 2213–2226, May 2015.
- [10] E. Arıkan, “A performance comparison of polar codes and Reed-Muller codes,” *IEEE Commun. Lett.*, vol. 12, pp. 447–449, June 2008.
- [11] A. Elkelesh, M. Ebada, S. Cammerer, and S. ten Brink, “Decoder-tailored polar code design using the genetic algorithm,” *IEEE Trans. Commun.*, vol. 67, pp. 4521–4534, July 2019.
- [12] Y. Liao, S. A. Hashemi, J. M. Cioffi, and A. Goldsmith, “Construction of polar codes with reinforcement learning,” *IEEE Trans. Commun.*, vol. 70, pp. 185–198, Jan. 2022.
- [13] S.-Y. Chung, *On the Construction of Some Capacity-Approaching Coding Schemes*. PhD thesis, MIT, 2000.
- [14] A. Ashikhmin, G. Kramer, and S. ten Brink, “Extrinsic information transfer functions: Model and erasure channel properties,” *IEEE Trans. Inform. Theory*, vol. 50, pp. 2657–2673, Nov. 2004.
- [15] S. ten Brink and G. Kramer, “Design of repeat-accumulate codes for iterative detection and decoding,” *IEEE Trans. Signal Process.*, vol. 51, pp. 2764–2772, Nov. 2003.
- [16] S. ten Brink, G. Kramer, and A. Ashikhmin, “Design of low-density parity-check codes for modulation and detection,” *IEEE Trans. Commun.*, vol. 52, pp. 670–678, Apr. 2004.
- [17] E. Sharon, A. Ashikhmin, and S. Litsyn, “EXIT functions for binary input memoryless symmetric channels,” *IEEE Trans. Commun.*, vol. 54, pp. 1207–1214, July 2006.
- [18] D. Divsalar, S. Dolinar, C. R. Jones, and K. Andrews, “Capacity-approaching protograph codes,” *IEEE J. Select. Areas Commun.*, vol. 27, pp. 876–888, Aug. 2009.
- [19] B. P. Smith, A. Farhood, A. Hunt, F. R. Kschischang, and J. Lodge, “Staircase codes: FEC for 100 Gb/s OTN,” *J. Lightw. Technol.*, vol. 30, pp. 110–117, Jan. 2012.
- [20] H. MahdaviFar and A. Vardy, “Achieving the secrecy capacity of wiretap channels using polar codes,” *IEEE Trans. Inform. Theory*, vol. 57, pp. 6428–6443, Oct. 2011.
- [21] K. Vakilinia, D. Divsalar, and R. D. Wesel, “RCA analysis of the polar codes and the use of feedback to aid polarization at short blocklengths,” in *Proc. 2015 IEEE Int. Symp. Inform. Theory (ISIT)*, pp. 1292–1296, June 2015.
- [22] D. Dosio, *Polar Codes For Error Correction: Analysis and Decoding Algorithms*. Laurea magistrale (master thesis), Università di Bologna, 2016.
- [23] F. Brännström, L. Rasmussen, and A. Grant, “Convergence analysis and optimal scheduling for multiple concatenated codes,” *IEEE Trans. Inform. Theory*, vol. 51, pp. 3354–3364, Sept. 2005.
- [24] A. Lozano, A. Tulino, and S. Verdu, “Optimum power allocation for parallel Gaussian channels with arbitrary input distributions,” *IEEE Trans. Inform. Theory*, vol. 52, pp. 3033–3051, July 2006.
- [25] R. M. Corless, G. H. Gonnet, D. E. G. Hare, D. J. Jeffrey, and D. E. Knuth, “On the Lambert W function,” *Adv. Comput. Math.*, vol. 5, pp. 329–359, Dec. 1996.